

AD-A286 209



NAVAL POSTGRADUATE SCHOOL
Monterey, California



THESIS

NOV 15 1994

INBAND SCATTERING FROM ARRAYS WITH
SERIES FEED NETWORKS

by

Seunghoon Lee

September 1994

Thesis Advisor:

David C. Jenn

Approved for public release; distribution is unlimited.

94-35205



DTIC QUALITY INSPECTED 5

94 11 15 003

REPORT DOCUMENTATION PAGE			Form Approved OMB No. 0704	
<p>Public reporting burden for this collection of information is estimated to average 1 hour per response, including the time for reviewing instruction, searching existing data sources, gathering and maintaining the data needed, and completing and reviewing the collection of information. Send comments regarding this burden estimate or any other aspect of this collection of information, including suggestions for reducing this burden, to Washington headquarters Services, Directorate for Information Operations and Reports, 1215 Jefferson Davis Highway, Suite 1204, Arlington, VA 22202-4302, and to the Office of Management and Budget, Paperwork Reduction Project (0704-0188) Washington DC 20503.</p>				
1. AGENCY USE ONLY (Leave Blank)		2. REPORT DATE September, 1994	3. REPORT TYPE AND DATES COVERED Master's Thesis, Final	
4. TITLE AND SUBTITLE INBAND SCATTERING FROM ARRAYS WITH SERIES FEED NETWORKS			5. FUNDING NUMBERS	
6. AUTHOR(S) Seunghoon Lee				
7. PERFORMING ORGANIZATION NAME(S) AND ADDRESS(ES) Naval Postgraduate School Monterey CA 93943-5000			8. PERFORMING ORGANIZATION REPORT NUMBER	
9. SPONSORING/MONITORING AGENCY NAME(S) AND ADDRESS(ES)			10. SPONSORING/MONITORING AGENCY REPORT NUMBER	
11. SUPPLEMENTARY NOTES The views expressed in this thesis are those of the author and do not reflect the official policy or position of the Department of Defense or the U S Government				
12a. DISTRIBUTION/AVAILABILITY STATEMENT Approved for public release. distribution unlimited			12b. DISTRIBUTION CODE A	
13. ABSTRACT Approximate formulas for the inband RCS of an array with series feed have been derived. The formulas are based on the hypothesis that an incident wave excites forward and backward traveling waves on the main line. The approximate formulas are in good agreement with results obtained using scattering matrices, thereby verifying the assumptions made in the approximate solution. Spikes in the RCS pattern have been identified with specific scattering sources in the array. The parameters affecting the level and location of the lobes have been noted. The main advantage of the approximate method relative to the scattering matrix method is its speed. The scattering matrix method requires that a matrix equation be solved, and its size increases with the number of array elements.				
14. SUBJECT TERMS Series feed antenna, RCS, Antenna RCS, Scattering Matrix			15. NUMBER OF PAGES 50	
			16. PRICE CODE	
17. SECURITY CLASSIFICATION OF REPORT Unclassified	18. SECURITY CLASSIFICATION OF THIS PAGE Unclassified	19. SECURITY CLASSIFICATION OF ABSTRACT Unclassified	20. LIMITATION OF ABSTRACT UL	

Approved for public release, distribution is unlimited.

INBAND SCATTERING FROM ARRAYS WITH SERIES FEED NETWORKS

by

Seunghoon Lee
CPT , Korean Army
B A , Korea Military Academy, March 1987

Submitted in partial fulfillment
of the requirements for the degree of

MASTER OF SCIENCE IN SYSTEMS ENGINEERING

from the

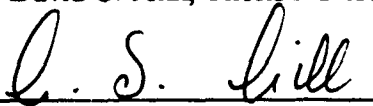
NAVAL POSTGRADUATE SCHOOL
September, 1994


Author


Seunghoon Lee

Approved By


David C. Jenn, Thesis Advisor


Gurnam S. Gill, Co-Advisor


Frederic H. Levien, Chairman
Electronic Warfare Academic Group

ABSTRACT

Approximate formulas for the inband RCS of an array with series feed have been derived. The formulas are based on the hypothesis that an incident wave excites forward and backward traveling waves on the main line. The approximate formulas are in good agreement with results obtained using scattering matrices, thereby verifying the assumptions made in the approximate solution. Spikes in the RCS pattern have been identified with specific scattering sources in the array. The parameters affecting the level and location of the lobes have been noted. The main advantage of the approximate method relative to the scattering matrix method is its speed. The scattering matrix method requires that a matrix equation be solved, and its size increases with the number of array elements.

Accession For	
NTIS GRA&I	<input checked="checked" type="checkbox"/>
DTIC TAB	<input type="checkbox"/>
Unannounced	<input type="checkbox"/>
Justification	
By	
Distribution/	
Availability Codes	
Dist	Avail and/or Special
A-1	

TABLE OF CONTENTS

I. INTRODUCTION	1
II. ANTENNA AND FEED SCATTERING ANALYSIS	4
A. DEFINITION OF RCS	4
B. ANTENNA SCATTERING	6
C. FEED REFLECTIONS	8
D. DERIVATION OF THE SERIES FEED RCS FORMULAS	13
III. COMPUTATION AND RESULTS	19
IV. CONCLUSION	27
APPENDIX A. COUPLING COEFFICIENTS.....	29
APPENDIX B. MATLAB PROGRAM LISTING	32
APPENDIX C. SCATTERING MATRIX FORMULATION	39
LIST OF REFERENCES	44
INITIAL DISTRIBUTION LIST	45

I. INTRODUCTION

Current state-of-the-art radars are sensitive enough to track small arms fire and even a swarm of insects. In response to this sensitivity, a higher standard of stealthy design has been employed to avoid detection by radar. The result has been radically stealthy platforms like the F-117A fighter and B-2 bomber. These are designed to have the smallest possible radar cross section (RCS), low infrared (IR) emissions, and low microwave emissions in order to avoid being detected and tracked.

The RCS of a target not only depends on the physical shape and material, but also on its sub-components such as antennas and other sensors. These components on the platforms must also be designed to meet low RCS requirements in addition to their sensor system requirements. In some cases the onboard sensors can be the predominant factor in determining a platform's total RCS. A typical example is a high gain antenna on a low RCS platform. If the antenna beam is pointed toward the threat radar and the threat frequency is in the antenna operating band, the antenna scattering can be significant.

Scattering from antennas has been the subject of interest since the 1950s. Extensive work has been done with regard to the determination of the antenna parameters [Ref.1], and dipole scattering and the effect of the terminal load impedance [Ref.2]. The RCS of horns [Ref.3], reflector antennas [Ref.4], and microstrip elements and arrays [Ref.5] have also been extensively studied. Detailed analysis of the inband scattering characteristics of arrays with parallel feed networks have also been investigated [Ref.6].

This thesis examines the scattering properties of phased arrays with series feed networks (Figure 1) which operate at the same frequency as that of the illuminating threat radar. For this so-called inband case, the threat signal will penetrate into the feed and be reflected at the mismatches and junctions of the array. This occurs even for a well-matched array because small mismatches exist within the feed. The total scattered power is a small fraction of the incident power, but for a large array, a large number of reflections exist which significantly contribute to the total RCS of the array. High performance arrays must ~~not~~ only meet the system operating requirements (i.e., high gain, low sidelobe levels, etc.) but also the RCS requirements. To ~~optimize the~~ tradeoff between antenna RCS and radiation performance, an efficient and accurate model of RCS is crucial. This thesis presents an approximate inband scattering model for arrays with series feeds. The approximate model is shown to be in good agreement with a more rigorous scattering matrix approach. The behavior of the RCS for various feed parameters is also determined.

Chapter II presents the theoretical background for the RCS analysis of the series-fed array antenna, and contains the derivation of the formulas for the approximate solution. Chapter III presents some computed data for both the approximate and rigorous solutions. Results ~~are also~~ presented to illustrate how the RCS is influenced by various feed parameters. Finally, Chapter IV summarizes the results of the data acquired and concludes with some design guidelines for controlling the behavior of the RCS. Some conclusions and recommendations are presented.

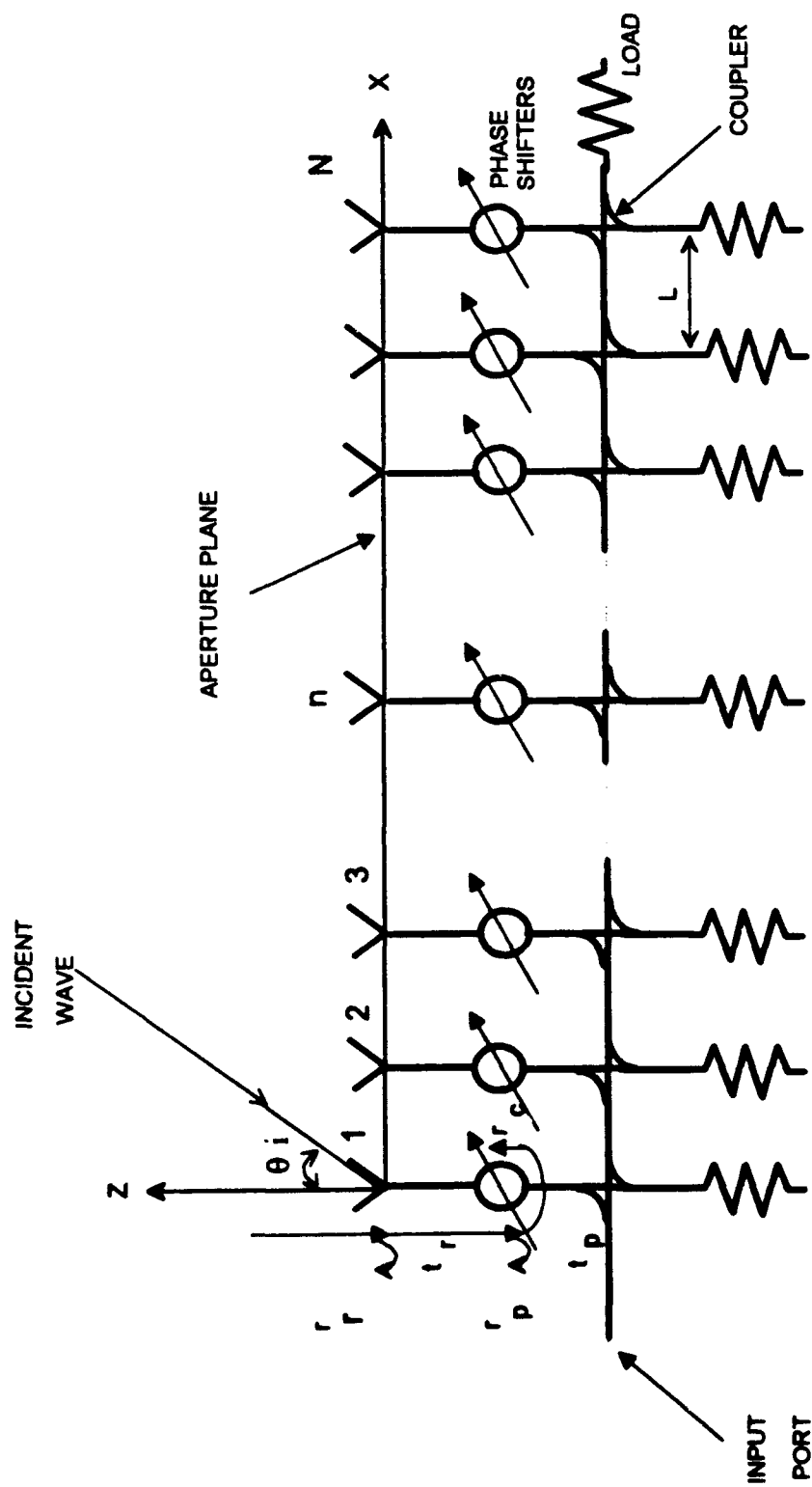


Figure 1 : Series feed antenna network.

II. ANTENNA AND FEED SCATTERING ANALYSIS

Scattered fields from a body are set up by a combination of induced electric and magnetic currents. The currents are induced such that the fields satisfy the boundary conditions and Maxwell's equations. The scattered field can be determined from the current using the radiation integrals. However, in most practical cases, determining the induced current is difficult or impossible. For a target such as an antenna the prediction of RCS is difficult because of many scattering sources both at the aperture and in the feed circuit. In fact, even antennas with identical amplitude and phase radiation patterns can differ in the way they scatter.

A. DEFINITION OF RCS

Radar cross section is a measure of power scattered by the target towards the illuminator. The definition of RCS can be stated as

$$\frac{\text{power reflected to receiver per unit solid angle}}{\text{incident power density} / 4\pi}.$$

In terms of the incident and scattered electric field intensities \vec{E}_i and \vec{E}_s , the RCS is

$$\sigma = \lim_{R \rightarrow \infty} 4\pi R^2 \frac{|\vec{E}_s|^2}{|\vec{E}_i|^2} \quad (1)$$

where R is the distance from the target to the observation point. In subsequent discussions only the monostatic RCS is considered. That is, the observation point is coincident with the transmit source. The limiting process in (1) assures that the incident wave is approximately a plane wave. Calculation of RCS is essentially a matter of finding the electric field scattered from a target. If the current induced on the target by the incident plane wave can be determined, then the radiation integrals used in antenna analysis can be applied to compute the scattered field. However, determining the induced current is a difficult problem because Maxwell's equations must be solved for complicated boundary conditions.

The unit of RCS most commonly used is decibels relative to a square meter (dBsm) which is computed by

$$\sigma, \text{ dBsm} = 10 \log(\sigma, m^2). \quad (2)$$

Radar cross section depends on many factors such as frequency and polarization of the incident wave, and the target orientation relative to the radar. RCS levels can range from 10,000 m^2 for ships to less than 0.001 m^2 for insects.

The scattering characteristics of a target are strongly dependent on the frequency of the incident wave. There are three frequency regions in which the RCS of a target is distinctly different. They are referred to as the low, resonance, and high-frequency regions, where low and high are defined relative to the size of the target in terms of incident wavelength, rather than their physical size. For a target of characteristic length L , the low-frequency

or Rayleigh region defined by $kL \ll 1$ ($k = 2\pi/\lambda$). The second is the resonance or Mie region where $kL \approx 1$. The last is the high-frequency region or the optical region defined by $kL \gg 1$. Depending on the threat radar's wavelength relative to the antenna's operating band, an arbitrary target can fall into either of the three regions.

B. ANTENNA SCATTERING ⁽¹⁾

The antenna's impact on RCS is twofold. First, the antenna frequently disturbs the continuity of the surface. This introduces more edges with a potential for increasing wide-angle scattering. A second aspect of the antenna scattering is that the threat radar's signal can penetrate into the feed and be reflected at internal mismatches and junctions. Even though these mismatches are small in the operating band, there can be a large number of scattering sources that add constructively under some conditions. This scattering is dependent on the type of feed and the devices incorporated therein.

The basic equation of antenna scattering has been presented by several authors [Ref. 2, 7-9]. The total scattered field for a linearly polarized antenna when the port is terminated with a load Z_L is

$$\vec{E}_s(Z_L) = \vec{E}_s(Z_a^*) + \left[\frac{j\eta}{4\lambda R_a} \vec{h} (\vec{h} \cdot \vec{E}_i) \frac{e^{-jkR}}{r} \right] \Gamma_o \quad (3)$$

⁽¹⁾ This discussion parallels that given in [Ref. 6].

where

$Z_a = R_a + jX_a$ is the radiation impedance

$R_a = R_r + R_d$ the antenna resistance

R_r = the radiation resistance

R_d = the ohmic resistance

\vec{h} = effective height

\vec{E}_i = incident field

$\eta = \sqrt{\mu/\epsilon}$ is the intrinsic impedance of the medium and,

$$\Gamma_o = \frac{Z_L - Z_a^*}{Z_L + Z_a^*} . \quad (4)$$

When the load impedance is the complex conjugate of the radiation impedance, Z_L is called a conjugate-matched load. In equation (3) $\vec{E}_i(Z_a^*)$ is the structural mode and the second term on the right-hand side is the antenna mode. When the antenna is conjugate matched, the antenna mode vanishes because the reflection coefficient Γ goes to zero. This can usually be achieved by having real values for the antenna impedance (i.e., "tuning out" its reactance), and connecting the terminals to a matched transmitter or receiver, thereby having no reflection at the junction between the antenna and the transmission line.

Kahn and Kurss [Ref. 10] found that for a dipole, conjugate matching results in half of the power being scattered and half absorbed. The reason being that for an isolated dipole, the structural mode is significant. If low RCS is desired, then it is necessary to mismatch the dipole terminals to

generate sufficient antenna mode to cancel the structural mode. Forcing the antenna mode term to zero by forcing Γ_0 to zero is impractical for large arrays because Z_a depends on angle and varies with element location in the array. However, it is possible in principal to reduce an array's RCS to low values. Green [Ref. 11] has shown that if a lossless, linearly polarized antenna absorbs more power than it scatters under matched conditions, its gain in the backward direction must exceed the forward direction gain. This condition is satisfied in the operating band of high-gain arrays.

C. FEED REFLECTIONS

In the case of an operational antenna, the incident threat signal power delivered to the radiating element terminals actually enters the feed network. The signal transmitted through the aperture elements is reflected at points inside of the feed circuit. For a phased array, the feed network can be extremely complicated, with potentially every transmission line discontinuity a source of reflected signals. In this thesis, the signal behavior in a series feed is examined.

A series feed is one in which the power to each element is tapped off of a main line sequentially, as illustrated in Figure 1. The coupling values are adjusted to provide the desired amplitude distribution. The most common method of terminating the main line is matched loading; another is to use a short which is called a standing wave feed. For the loaded case, some power is always reflected from the load at the end of the main line which gives rise to a "reflection lobe" in the radiation pattern. It is reduced in magnitude

relative to the main beam by an amount determined by the load reflection coefficient.

There are two antenna scattering modes to consider in the calculation of RCS. The first is the antenna or radiation mode which is determined by the radiation properties of the antenna and it vanishes when the antenna is conjugate matched to its radiation impedance. The second mode is the structural mode that is generated by the induced currents on the antenna surfaces. This thesis only examines the antenna mode which is the dominant RCS contribution to a phased array in the operating band.

Total RCS can be computed by summing the scattering from all the signals that enter the array, are reflected by the mismatches of the components, and then return to the aperture. The RCS is obtained from combining equations (1) and (3) over all the array elements [Ref. 6]

$$\sigma(\theta, \phi) = \frac{4\pi A_e^2}{\lambda^2} \left| \sum_{n=1}^N \Gamma_n(\theta, \phi) e^{j \vec{k} \cdot \vec{d}_n} \right|^2 |F_{norm}(\theta, \phi)|^2 \quad (5)$$

where

$\Gamma_n(\theta, \phi)$ = total reflected signal returned to the aperture for element n

when the wave is incident from the (θ, ϕ) direction

$\vec{k} = k(u\hat{x} + v\hat{y} + w\hat{z})$ = wave vector

$u = \sin \theta \cos \phi$

$v = \sin \theta \sin \phi$

$w = \cos \theta$

\vec{d}_n = position vector to element n

A_e = effective area of an element = $h^2 Z_o / 4 R_a$

F_{norm} = normalized element scattering pattern.

There are two approaches to obtaining Γ in equation (5). One is to use a network matrix method such as scattering parameters. All interactions between the feed devices are included. The scattering matrix approach is computationally intense because a matrix equation must be solved. As N increases the size of the matrix increases. A second approach is to trace signals through the feed. However, tracing the signal flow inside a feed network can be extremely difficult and tedious job, and to include all the multiple reflections for accurate calculation is even more difficult. For inband cases where the reflection coefficients of the devices are small ($r \ll 1$), higher order reflections can be neglected. The following approximations are made for the simplified analysis [Ref.12] :

1. Devices of the same type are assumed to have identical electrical characteristics. For example, all of the radiating elements have the same reflection and transmission coefficients (r_r and t_r), with the exception of phase shifters which have a transmission coefficient of the form

$$t_{p_n} = t_p e^{j\chi_n}$$

where

$$\begin{aligned}\chi_n &= (n-1)\alpha_s, \\ \alpha_s &= k_o d_x \sin \theta_s \cos \phi_s = k_o d_x u_s, \\ (\theta_s, \phi_s) &= \text{the direction of the array radiation beam.}\end{aligned}$$

Note that the magnitude of the transmission coefficient is the same for all phase shifters : $|t_{p_n}| = t_p$.

2. The feed devices are well matched so that $r \ll 1$ and therefore higher order reflections can be neglected.

3. Lossless devices will be assumed,

$$|r|^2 + |t|^2 = 1.$$

With the previous assumptions, the fraction of signal entering the radiating elements that is reflected back to the aperture for reradiation is

$$\begin{aligned} \Gamma_n = & r_r e^{j(n-1)\alpha} + t_r^2 r_p e^{j(n-1)\alpha} + t_r^2 t_p^2 r_c e^{j2(n-1)\alpha} e^{j(n-1)\alpha} \\ & + t_r^2 t_p^2 e^{j(n-1)\alpha} E'_n. \end{aligned} \quad (6)$$

where

$\alpha = k_0 d_x u$ is the incident wave inter-element space delay
 $u = \sin \theta \cos \phi,$

E'_n represents the signal re-emerging from the series feed at element n . As will be seen later, some of this signal is due to elements toward the input ($m < n$), some due to elements toward the termination ($m > n$), and some due to the load at the coupler n .

Equation (6) shows that the total scattered field is a sum of scattering patterns from each mismatch group in the feed

$$|E^s| = |E_r^s + E_p^s + E_c^s + E_s^s|. \quad (7)$$

E_s^s is the total scattered field due to the series feed reflections. It is obtained by summing over all E_n^s as described in the next section. Assuming that only one scattering peak dominates at any given incident angle, it may be sufficient to approximate the magnitude squared of the sum in (7) by the sum of the magnitudes squared

$$|E^s|^2 \approx |E_r^s|^2 + |E_p^s|^2 + |E_c^s|^2 + |E_s^s|^2. \quad (8)$$

The RCS contribution from the radiating element, phase shifters and coupler inputs are [Ref. 13]

$$\sigma_r \approx \frac{4\pi A^2 \cos^2 \theta}{\lambda^2} r_r^2 \left[\frac{\sin(N\alpha)}{N \sin(\alpha)} \right]^2 \quad (9)$$

$$\sigma_p \approx \frac{4\pi A^2 \cos^2 \theta}{\lambda^2} r_p^2 t_r^4 \left[\frac{\sin(N\alpha)}{N \sin(\alpha)} \right]^2 \quad (10)$$

$$\sigma_c \approx \frac{4\pi A^2 \cos^2 \theta}{\lambda^2} r_c^2 t_r^4 t_p^4 \left[\frac{\sin(N\zeta)}{N \sin(\zeta)} \right]^2 \quad (11)$$

where $\zeta = \alpha + \alpha_s$.

D. DERIVATION OF THE SERIES FEED RCS FORMULAS

Figure 2 shows the signal distribution for the n^{th} four port coupler with coupling coefficient c_n and transmission coefficient t_n . To begin with, the

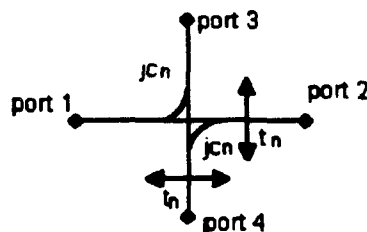


Figure 2: Coupling and transmission paths for a four port coupler.

couplers are assumed lossless, matched and to have perfect isolation between the coupled port and through port. The scattering matrix is

$$\mathbf{c}_n = \begin{bmatrix} 0 & t_n & j c_n & 0 \\ t_n & 0 & 0 & -j c_n \\ j c_n & 0 & 0 & t_n \\ 0 & -j c_n & t_n & 0 \end{bmatrix} \quad (12)$$

To obtain formulas for the feed reflections, the received incident threat signal can be decomposed into forward and backward traveling waves on the main line. Figure 3 shows that a signal received by element n appears as an excitation for the $N - n$ elements toward the load and the $n - 1$ elements toward the input. Other scattering terms not included in the forward or backward beam are the “self-reflected beam” due to the reflection from the

load terminating element n , and the “input load reflected beam” due to the reflection from the input load or receiver at the beginning of the feed. Thus for each element in the array four beams are reradiated, and their beamwidths and peak levels depend on the element location in the array. The total scattered field is obtained by the superposition of the forward, backward, self-reflected, and input load reflected beams from all elements.

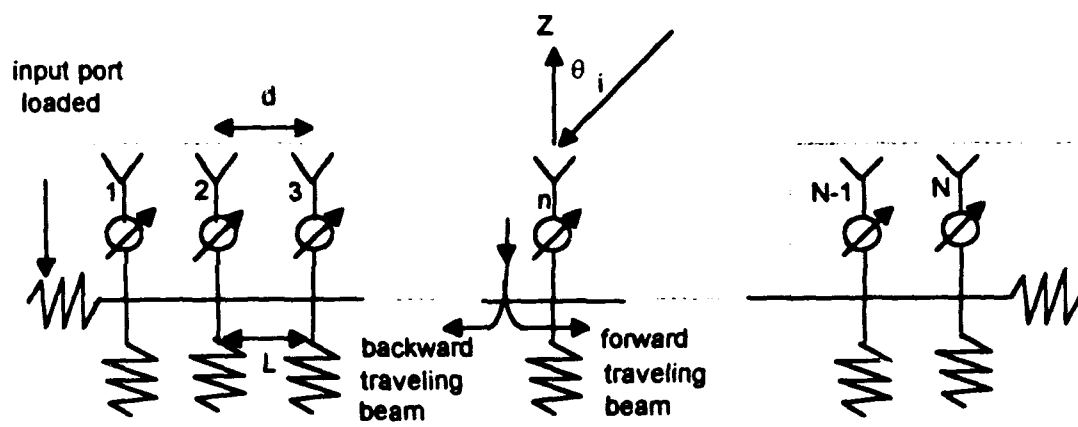


Figure 3 : Forward and backward traveling waves in a series feed network.

The formulas for the RCS of the series network can be obtained by tracing signals through the feed. Let Γ_L be the reflection coefficient of all of the loads. For an incident signal at element n , “forward wave” that travels toward element N (see Figure 4), radiates reflected signals from $n+1$ up to element N and can be expressed as ⁽²⁾

(2) The expressions for the electric field intensity (E) have the leading constants and free space Green's function omitted because only a ratio is needed in Equation (1).

$$\begin{aligned}
E_{f_n} = & e^{j(n-1)(\alpha_s + \alpha)} j c_n \Gamma_L t_n \{ e^{j\psi_o} j c_{n+1} e^{jn(\alpha_s + \alpha)} \\
& + e^{j2\psi_o} t_{n+1} j c_{n+2} e^{j(n+1)(\alpha_s + \alpha)} + \dots \\
& + e^{j(N-n)\psi_o} t_{n+1} t_{n+2} \dots t_{N-1} j c_N e^{j(N-1)(\alpha_s + \alpha)} \}, \quad (13)
\end{aligned}$$

where $\psi_o = kL$. The electrical line length between couplers is denoted as ψ_o and it is equal to k times the physical length of the line. The “backward wave” that travels toward the input (see Figure 5), radiates reflected signals from the $n-1$ elements downline from element n

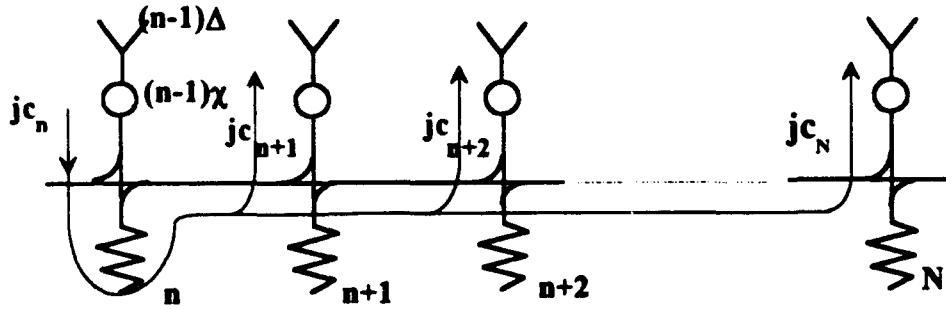


Figure 4 : Forward wave (traveling toward element N).

$$\begin{aligned}
E_{b_n} = & \Gamma_L e^{j(n-1)(\alpha_s + \alpha)} \{ t_n^2 e^{j(n-1)(\alpha_s + \alpha)} + j c_n j c_{n-1} t_{n-1} e^{j\psi_o} e^{j(n-2)(\alpha_s + \alpha)} \\
& + j c_n (t_{n-1} e^{j\psi_o}) j c_{n-2} e^{j\psi_o} t_{n-2} e^{j(n-3)(\alpha_s + \alpha)} + \dots \\
& + j c_{n-1} e^{j\psi_o} \left(\prod_{i=2}^{n-1} t_i e^{j\psi_o} \right) j c_1 t_1 e^{j \cdot 0 (\alpha_s + \alpha)} \}. \quad (14)
\end{aligned}$$

The self-reflection is due to the load at coupler n , and it is unique in its form. Thus it can be separated and simplified as

$$E_{self_n} = \Gamma_L t_n^2 e^{j 2(n-1)(\alpha_s + \alpha)} . \quad (15)$$

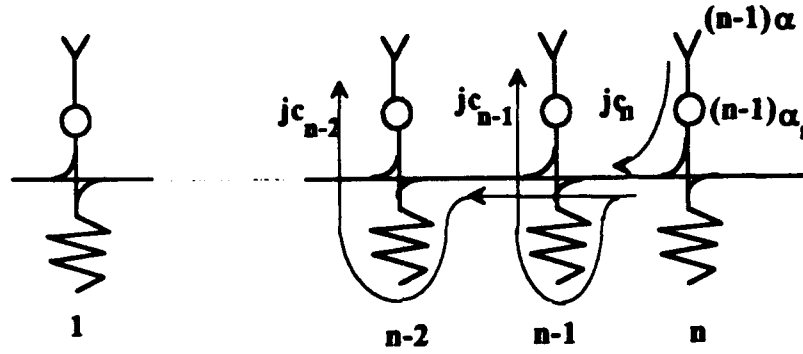


Figure 5 : Backward wave (traveling toward element 1 - input).

For the reflection from the input load , the equation is given by

$$E_{in_n} = j c_n e^{j(n-1)(\alpha + \psi_o)} \left[\prod_{m=1}^{n-1} t_m \right] \Gamma_o . \quad (16)$$

The total forward, self, input load, and backward traveling fields from all the elements caused by an incident wave is obtained by summing over all elements

$$E_f = -\Gamma_L \sum_{n=1}^{N-1} c_n e^{j(n-1)\zeta} \left\{ \sum_{m=n+1}^N c_m e^{j(m-1)\zeta} \left(\prod_{i=1}^{m-1} t_i e^{j\psi_0} \right) \right\}, \quad (17)$$

$$E_b = -\Gamma_L \sum_{n=2}^{N-1} c_n e^{j(n-1)\zeta} \left\{ \sum_{m=1}^{n-1} c_m e^{j(m-1)\zeta} \left(\prod_{i=m}^{n-1} t_i e^{j\psi_0} \right) \right\}, \quad (18)$$

$$E_{in} = -\Gamma_0 t_r^2 t_p^2 \left\{ \sum_{n=1}^N c_n e^{j(n-1)(\zeta+\psi)} \left(\prod_{m=1}^{n-1} t_m \right) \right\}^2, \quad (19)$$

$$E_{self} = \sum_{n=1}^N \Gamma_L t_n^2 e^{j2(n-1)\zeta}. \quad (20)$$

The minus sign occurs for some terms because the reflected beams pass through two coupled arms yielding a j^2 factor. The total scattered field due to the series feed beam is

$$\begin{aligned} |E_s^s|^2 &= |E_f + E_b + E_{in} + E_{self}|^2 \\ &\approx |E_f|^2 + |E_b|^2 + |E_{in}|^2 + |E_{self}|^2 \end{aligned} \quad (21)$$

The correct normalization can be obtained by comparing the total scattered field in equation (21) to the maximum that would be obtained by an array with completely reflecting elements ($=N$). Thus

$$\sigma_s \approx \frac{4\pi A^2 \cos^2 \theta}{\lambda^2} t_r^4 t_p^4 \left| \frac{E_i}{N} \right|^2. \quad (22)$$

The coupling coefficients (c_n) are determined by the prescribed radiation beam sidelobe level. Appendix A describes how the coefficients are computed from a given amplitude distribution.

III. COMPUTATION AND RESULTS

In this chapter, calculated results are presented for series fed arrays using equations (17) through (22). To verify the approximate method, data is compared with the rigorous method using scattering matrices. The scattering matrix solution is described briefly in Appendix C. The aperture element is represented by a two-port device with the reflection coefficient r_r , allowing direct comparison between both approximate and scattering matrix solutions. This provides a means of evaluating the validity of the assumptions made in deriving the approximate equations.

For the series-fed phased array with series feed network operating at wavelength λ , calculations were performed for the parameter sets listed in Table 1.

TABLE 1 : SERIES-FED PHASED ARRAY PARAMETERS.

parameter	range
no. of elements, N	50
ψ_0	$0, \pi/4, \pi/2, \pi$
d	0.4λ
r_r, r_p, r_c	0.2
l	0.5λ
c_m	uniform, cosine-squared on a pedestal
θ_s	$0^\circ, 45^\circ$

A MATLAB program for calculating the approximate RCS is shown in Appendix B. Each element of the array (Figure 1) that is illuminated by the incident wave has its own forward wave, backward, self and input reflected term as discussed in Chapter II, Section D.

Some parameters are varied to study the behavior of RCS. They include the scan angle (θ_s), the line length between couplers (ψ_o), and the coupling coefficients (c_m). Figures 6 and 7 show the difference between the broadside and scanned RCS when $\psi_o = \pi/4$. It can be observed that the highest spike at $\theta = 0^\circ$ on both graphs is due to specular scattering from the radiating elements. The spikes at about -20° in Figure 6 and at 20° in Figure 7 are due to the reflection from the input load. The spike at -35° in Figure 7 is due to Bragg diffraction, and the one at 45° is due to the effects of forward and backward waves on the main line scattering retrodirectively. A comparison of the scanned and broadside cases shows that the reflections

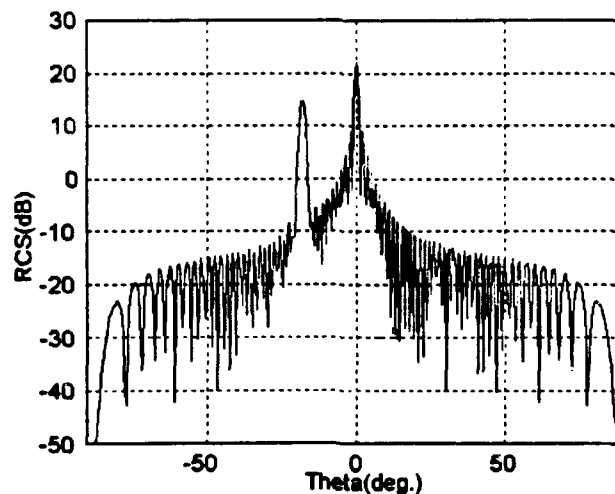


Figure 6 : RCS of series fed array by the approximate method.

$$(\theta_s = 0^\circ, \psi_o = \pi/4)$$

from points behind the phase shifters move toward or away from the specular beam along with the array's radiation beam.

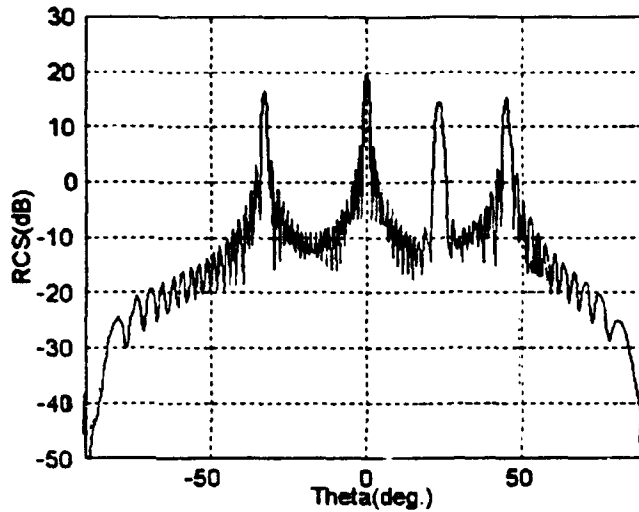


Figure 7 : RCS of series fed array by the approximate method.

$$(\theta_s = \pi/4, \psi_s = \pi/4)$$

In general, the individual spikes can be attributed to specific scattering sources in the antenna. The specular reflection (due to r_r) has its peak at $\theta = 0^\circ$. There are no Bragg lobes for this term because the element spacing is sufficiently small. Reflections from the input of the phase shifter have a similar behavior as can be seen from equation (10). Reflected signals from the coupler inputs will pass through the phase shifter and therefore scan along with the radiation beam. (This can be a problem for an array on a stealthy platform if it is used to track a threat.) When the array is scanned, a second lobe due to Bragg diffraction moves into the visible region.

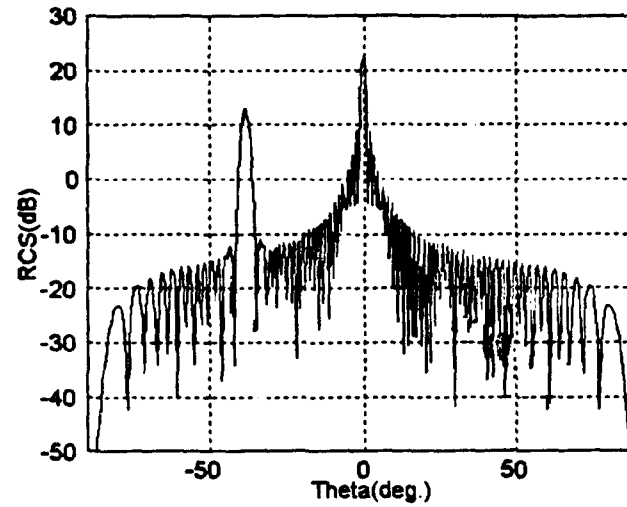


Figure 8 : RCS of series fed array by the approximate method.

$$(\theta_s = 0^\circ, \psi_s = \pi/2)$$

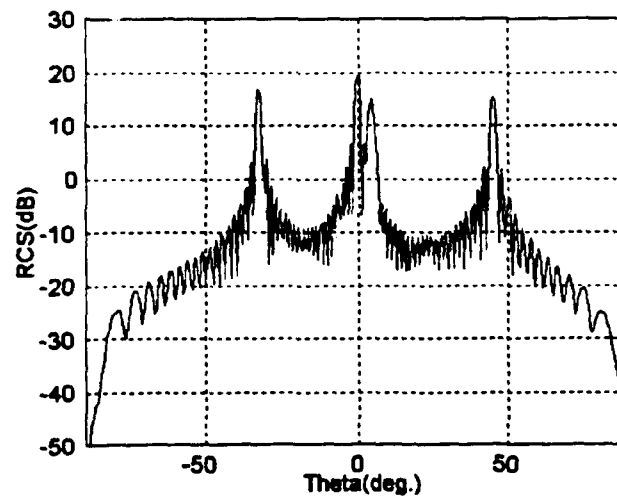


Figure 9 : RCS of series fed array by the approximate method.

$$(\theta_s = \pi/4, \psi_s = \pi/2)$$

A large lobe also arises due to the reflection from the input load. In this case, the array acts as a receive antenna that collects the incident threat signal. A portion of this signal is reflected at the terminals and appears just as if a transmit signal has been injected into the antenna. Thus the RCS pattern is the gain pattern squared. It can be seen by comparing Figures 6, 7 and 9 that the lobe from the input load reflection is determined by ψ_0 as well as θ_0 .

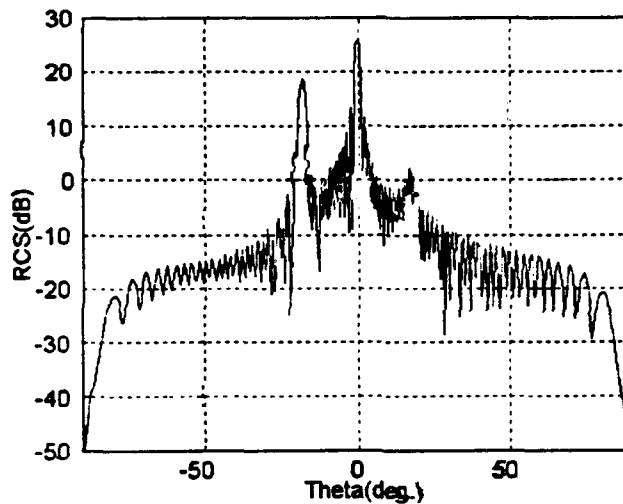


Figure 10 : RCS of a series fed array by the scattering matrix method.

$$(\theta_0 = 0^\circ, \psi_0 = \pi/4)$$

The RCS patterns obtained using the scattering matrix method are shown in Figures 10 through 13. They correspond to the same cases shown in Figures 6 through 9. This solution can be considered rigorous in the sense that all interactions and multiple reflections are included. The agreement between the approximate and the rigorous solution is excellent.

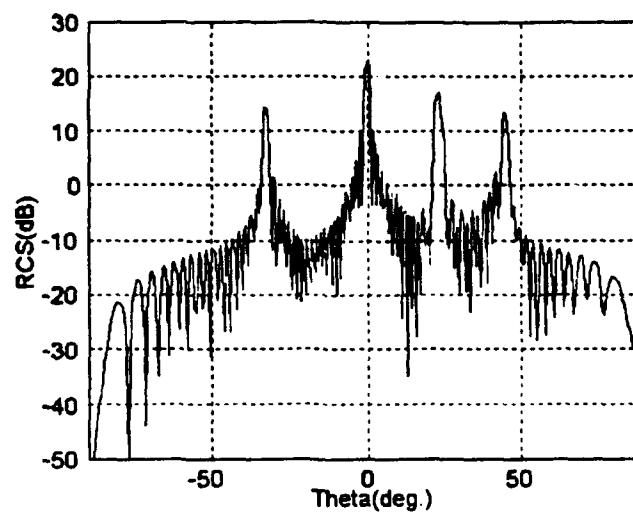


Figure 11 : RCS of a series fed array by the scattering matrix method.

$$(\theta_s = \pi/4, \psi_s = \pi/4)$$

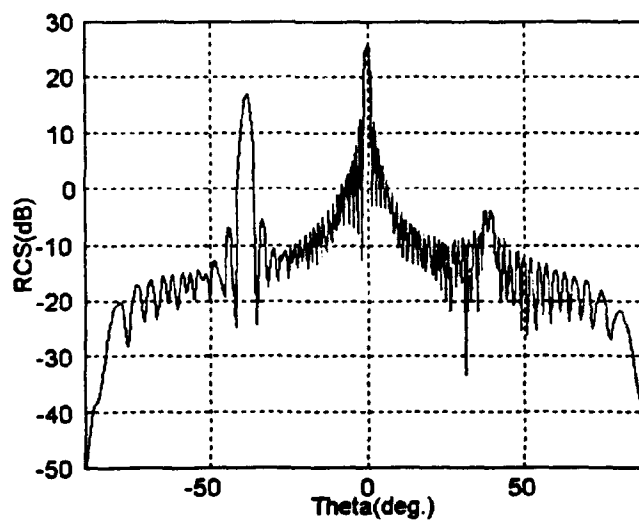


Figure 12 : RCS of a series fed array by the scattering matrix method.

$$(\theta_s = 0^\circ, \psi_s = \pi/2)$$

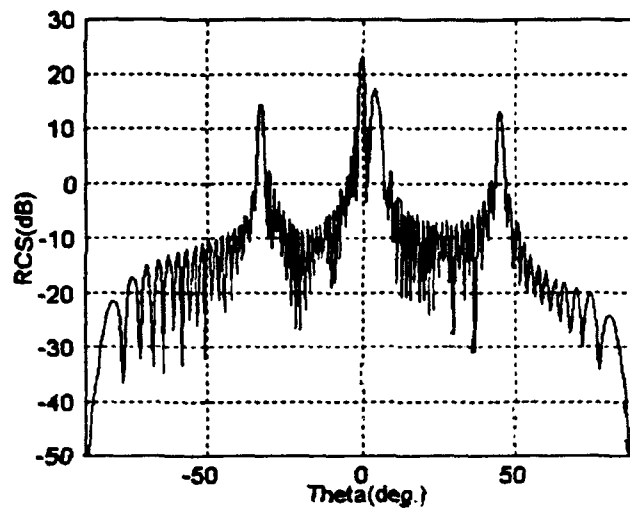


Figure 13 : RCS of a series fed array by the scattering matrix method.

$$(\theta_s = \pi/4, \psi_s = \pi/2)$$

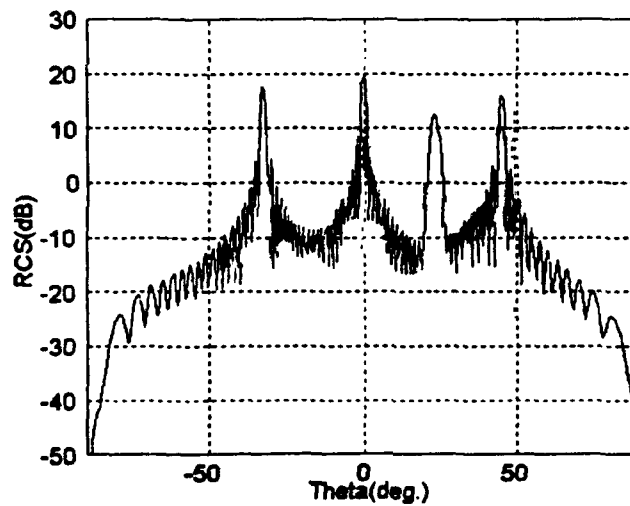


Figure 14 : RCS of a series fed array with tapered amplitude distribution by the approximate method $(\theta_s = \pi/4, \psi_s = \pi/2)$.

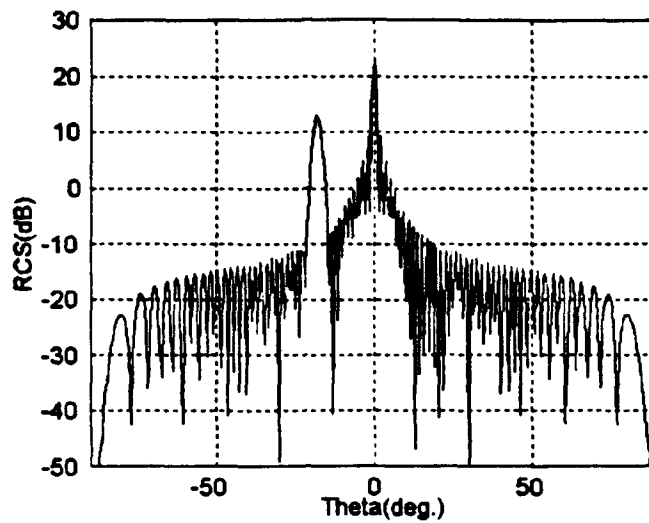


Figure 15 : RCS of a series fed array with tapered amplitude distribution by the approximate method ($\theta_s = 0^\circ$, $\psi_s = \pi/2$).

The effects of changing the coupling distribution is illustrated in Figures 14 and 15. The RCS behavior is essentially the same but the feed contributions to RCS are reduced slightly.

IV. CONCLUSION

Approximate formulas for the inband RCS of an array with series feed have been derived. The formulas are based on the hypothesis that an incident wave excites forward and backward traveling waves on the main line. The approximate formulas are in good agreement with results obtained using scattering matrices, thereby verifying the assumptions made in the approximate solution.

Spikes in the RCS pattern have been identified with specific scattering sources in the array. The parameters affecting the level and location of the lobes have been noted. By properly choosing parameters such as ψ_0 and Γ_L , it is possible to control the spikes to some extent. The data shows that there is no preferred value of ψ_0 that eliminates the input load reflection. It is common practice that the line length between couplers should be set to an odd multiple of a quarter wavelength to cancel multiple reflections. However, total suppression of the RCS can only be achieved by perfectly matching all of the feed devices, which is practically impossible.

The main advantage of the approximate method relative to the scattering matrix method is its speed. The scattering matrix method requires that a matrix equation be solved, and its size increases with the number of array elements. A typical approximate calculation takes about 2 min. on a Sparc 10, whereas the matrix solution runs about 2 hours (50 elements and 0.5° increments). Also, the approximate formulas are easily extended to an arbitrary number of elements. Since both methods assume lossless feed

networks and identical reflection coefficients for all similar devices, the actual value of RCS can be expected to be slightly lower than shown.

For future research, it is recommended that the RCS of a two-dimensional array be investigated and be presented in contour form [Ref. 6]. The RCS of hybrid feed networks (e.g., series fed in one dimension and parallel fed in the other) should also be examined.

APPENDIX A : COUPLING COEFFICIENTS

This appendix derives the series feed coupling coefficients for a given amplitude distribution $\{a_n\}$. For uniform illumination (13dB sidelobe level) $a_n = 1$, $n=1, 2, \dots, N$ where N is the number of couplers. Also of interest is a cosine-squared on a pedestal distribution (32dB sidelobe level) where

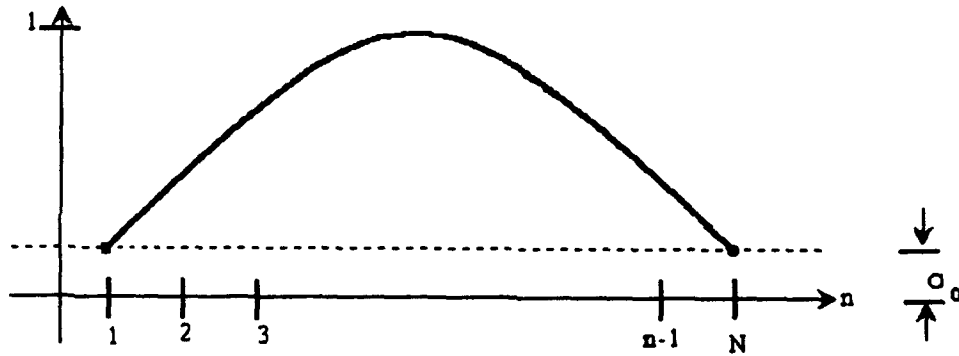


Figure A.1 : Cosine-squared distribution.

$$a_n = a_o + (1 - a_o) \sin^2 \left(\frac{n-1}{N-1} \times \pi \right)$$

and $a_o = 0.2$, as illustrated in Figure A.1. Referring to Figure A.2, for a lossless feed

$$P_{in} = \sum_{n=1}^N k a_n^2 + P_L$$

or,

$$P_{in} - P_L = k \sum_n a_n^2$$

and

$$k = \frac{P_{in} - P_L}{\sum_n a_n^2} \xRightarrow{P_{in}=1} \frac{1 - P_L}{\sum_n a_n^2}.$$

Note that P_L is the power into the load and P_{in} is the total input power.

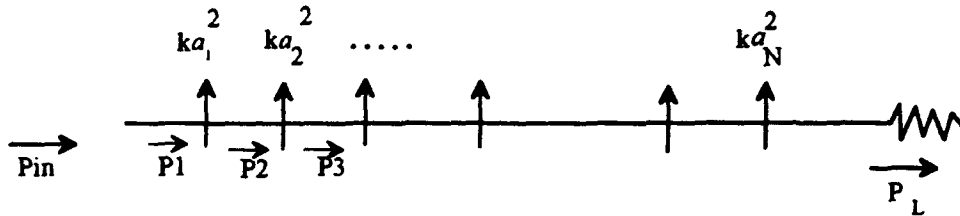


Figure A.2 : Power into the lossless feed.

The coupling coefficients are defined by

$$c_m^2 = \frac{ka_m^2}{P_m}$$

where

$$P_m = P_{in} - \sum_{q=1}^{m-1} ka_q^2 = 1 - \sum_{q=1}^{m-1} ka_q^2.$$

Therefore, for unit power into the load ($P_{in}=1$), the coupling coefficient becomes

$$c_m^2 = \frac{ka_m^2}{P_{in} - \sum_{q=1}^{m-1} ka_q^2} = \frac{a_m^2}{\frac{1}{k} - \sum_{q=1}^{m-1} a_q^2} = \frac{a_m^2}{\frac{1}{1-P_L} \sum_{n=1}^N a_n^2 - \sum_{n=1}^{m-1} a_n^2} .$$

The transmission coefficients are given by

$$t_m^2 = 1 - c_m^2 .$$

APPENDIX B : MATLAB PROGRAM LISTING

This appendix presents a listing of the MATLAB Code that computes the RCS using the approximate formulas. The version listed is for uniform amplitude distribution and no scan.

```
%% INBAND SCATTERING FROM ARRAYS WITH SERIES FEED NETWORKS
%% Approximate Method (Broadside RCS Uniform Distribution).
```

```
N=50,,      Gamma=0.2,,      Si=pi/4;
Ao=1,,      Pl=0.05,,      ki=0.8*pi*sin(0);
theta=-pi/2:pi/360:pi/2,,      theta1=theta.*180/pi;
```

```
% a) Forward Wave : (Travels toward element N)
```

```
for a=1:N;
    A(a)=Ao+((1-Ao)*(sin(((a-1)/(N-1)).*pi)).^2);
end
```

```
for l=1:N;
    Cm(l)=sqrt((A(max(l))^2)/(((1/(1-Pl))*(sum(A(1:N).^2)))-(sum(A(1:l-1).^2)))
);
end
```

```

for i=1:N-1;
    t1(i)=((sqrt(1-(Cm(max(i)).^2))).*exp(j*Si));
    t2(i)=(sqrt(1-(Cm(max(i)).^2)));
end

for k=1:N;
    tsf(k)=(1-(Cm(max(i)).^2));
    t3(k)=prod(t1(1:k-1));
    t4(k)=prod(t1(1:k-2));
    t5(k)=prod(t2(1:k-1));
end

for z=1:361;
    del1(z)=sin(theta(max(z))).*(0.8*pi);
    del=del1(max(z));
    for n=1:N-1;
        for m=n+1:N;
            Ef5(m)=Cm(m).*exp(j*(m-1)*(ki+del))*t3(m);
        end
        Ef4=sum(Ef5);
        Ef3(n)=Cm(n).*exp(j*(n-1)*(ki+del))*Ef4;
    end
    Ef2=sum(Ef3);
    Ef1(z)=-Gamma*Ef2;

```

% b) Self term :

for p=1:N;

$Esf3(p) = \Gamma * tsf(p) * \exp(j * 2 * (p-1) * (k_i + \Delta))$;

end

$Esf2 = \sum(Esf3)$;

$Esf1(z) = (Esf2)$;

% c) Backward Wave : (Travels toward element 1-input)

for q=2:N-1;

 for r=1:q-1;

$Eb5(r) = C_m(r) * \exp(j * (r-1) * (k_i + \Delta)) * t4(r)$;

 end

$Eb4 = \sum(Eb5)$;

$Eb3(q) = C_m(q) * \exp(j * (q-1) * (k_i + \Delta)) * Eb4$;

end

$Eb2 = \sum(Eb3)$;

$Eb1(z) = -\Gamma * Eb2$;

% d) Input load reflected wave

for s=1:N

$Ein3(s) = C_m(s) * \exp(j * (s-1) * (k_i + \Delta + S_i)) * t5(s)$;

end

```

Ein2=sum(Ein3);
Ein1(z)=-Gamma*(1-Gamma^2)^2*(Ein2).^2;
end

Ef(:)=10.*log10(abs(Ef1(:)));
Esf(:)=10.*log10(abs(Esf1(:)));
Eb(:)=10.*log10(abs(Eb1(:)));
Ein(:)=10.*log10(abs(Ein1(:)));

Es=(abs(Ef1)).^2+(abs(Esf1)).^2+(abs(Eb1)).^2+(abs(Ein1)).^2;
En1=Es./(N^2);

for s=1:361;
    if sin(dell(max(s)))==0
Rf(s)=1;
    else
Rf(s)=(sin(N*dell(max(s)))/(N.*sin(dell(max(s)))).^2;
    end
    if sin(0.8*pi*(sin(theta(max(s)))+sin(0)))==0
Rfs(s)=1;
    else
Rfs(s)=(sin(N*0.8*pi*(sin(theta(max(s)))+sin(0)))/(N.*sin(0.8*pi*(sin(theta(
max(s)))+sin(0))))).^2;
    end
end
end

```



```

for t=1:361;
RCS1(t)=(400*pi*(cos(theta(max(t))))^2).*(1-Gamma^2)^4.*En1(t);
RCSr(t)=(400*pi*(cos(theta(max(t))))^2).*Gamma^2.*Rf(max(t));
RCSp(t)=(400*pi*(cos(theta(max(t))))^2).*Gamma^2*(1-Gamma^2)^2.*Rf(
max(t));
RCSc(t)=(400*pi*(cos(theta(max(t))))^2).*Gamma^2*((1-Gamma^2)^4.*Rfs
(max(t)));
end

RCS2(:)=10.*log10((RCS1(:))+1.e-10);
RCSR(:)=10.*log10((RCSr(:))+1.e-10);
RCSP(:)=10.*log10((RCSp(:))+1.e-10);
RCSC(:)=10.*log10((RCSc(:))+1.e-10);

RCSt=RCS1+RCSR+RCSp+RCSc;
RCS(:)=10.*log10((RCSt(:))+1.e-10);

figure
plot(theta1,Ef),    grid,  axis([-90 90 -50 30]);
title('Forward wave vs Angle')
xlabel('Theta(deg)'),    ylabel('Ef(dB)')
pause

```

```
figure
plot(theta1,Esf), grid, axis([-90 90 -50 30]);
title('Self-Reflected wave vs Angle')
xlabel('Theta(deg.)'), ylabel('Esf(dB)')
pause
```

```
figure
plot(theta1,Eb), grid, axis([-90 90 -50 30]);
title('Backward wave vs Angle')
xlabel('Theta(deg.)'), ylabel('Eb(dB)')
pause
```

```
figure
plot(theta1,Ein), grid, axis([-90 90 -50 30]);
title('Load reflected wave vs Angle')
xlabel('Theta(deg.)'), ylabel('Ein(dB)')
pause
```

```
figure
subplot(221), plot(theta1,RCS2)
grid, axis([-90 90 -50 30]);, title('Ant. RCS vs Angle')
xlabel('Theta(deg.)'), ylabel('RCS(dB)')
pause
```

```

subplot(222),      plot(theta1,RCSR)
grid              axis([-90 90 -50 30]);,  title('Reflected RCS vs Angle')
xlabel('Theta(deg)'),  ylabel('RCS(dB)')
pause

subplot(223),      plot(theta1,RCSP)
grid              axis([-90 90 -50 30]);,  title('Phase Shifter RCS vs Angle')
xlabel('Theta(deg)'),  ylabel('RCS(dB)')
pause

subplot(224),      plot(theta1,RCSC)
grid              axis([-90 90 -50 30]);,  title('Coupler RCS vs Angle')
xlabel('Theta(deg)'),  ylabel('RCS(dB)')
pause

figure
plot(theta1,RCS),      grid
axis([-90 90 -50 30]);,  title('Total RCS vs Angle')
xlabel('Theta(deg)'),  ylabel('RCS(dB)')
save rcsbn2 theta1 RCS Ef Esf Eb Ein RCS2 RCSR RCSP RCSC
pause,      axis;,      end

```

APPENDIX C : SCATTERING MATRIX FORMULATION

The series feed is represented by an interconnection of two and four port devices as shown in Figure C.1. The unknown quantities are the set of $\{a_n\}$. A scattering equation can be written at each port. Thus for an N element array, there are $8N$ equations that must be solved simultaneously.

The scattering matrix of the radiating element is

$$d = \begin{bmatrix} d_{11} & d_{12} \\ d_{21} & d_{22} \end{bmatrix} = \begin{bmatrix} r_r & t_r \\ t_r & r_r \end{bmatrix}.$$

For the phase shifter

$$p_n = \begin{bmatrix} (p_n)_{11} & (p_n)_{12} \\ (p_n)_{21} & (p_n)_{22} \end{bmatrix} = \begin{bmatrix} r_p & t_p e^{j(n-1)\alpha_s} \\ t_p e^{j(n-1)\alpha_s} & r_p \end{bmatrix}.$$

The excitations are due to the incident plane where $S_n = e^{j(n-1)\alpha}$.

Starting with element 1, the two scattering equations at the radiating devices are

$$a_1 = S_1 d_{11} + a_3 d_{12} \quad (1)$$

$$a_2 = S_1 d_{21} + a_3 d_{22} \quad (2)$$

and at the phase shifter ports

$$a_3 = a_2(p_1)_{11} + a_5(p_1)_{12} \quad (3)$$

$$a_4 = a_2(p_1)_{21} + a_5(p_1)_{22} \quad (4)$$

Four equations can be written at coupler 1 (c_1)

$$a_6 = a_6 \Gamma(c_1)_{11} + \psi a_9(c_1)_{12} + a_4(c_1)_{13} + a_7 \Gamma(c_1)_{14} \quad (5)$$

$$a_8 = a_6 \Gamma(c_1)_{21} + \psi a_9(c_1)_{22} + a_4(c_1)_{23} + a_7 \Gamma(c_1)_{24} \quad (6)$$

$$a_5 = a_6 \Gamma(c_1)_{31} + \psi a_9(c_1)_{32} + a_4(c_1)_{33} + a_7 \Gamma(c_1)_{34} \quad (7)$$

$$a_7 = a_6 \Gamma(c_1)_{41} + \psi a_9(c_1)_{42} + a_4(c_1)_{43} + a_7 \Gamma(c_1)_{44} \quad (8)$$

It has been assumed that all loads are identical ($\Gamma_0 = \Gamma_1 = \dots = \Gamma_N \equiv \Gamma$). Similarly, all interelement line lengths are equal ($\psi_1 = \psi_2 = \dots = \psi_N \equiv \psi = e^{jkL}$). The coupling coefficients are given in Appendix A and the scattering matrix by equation (12).

For elements 2 through N, a pattern repeats. At the radiating element

$$a_{8n-6} = S_n d_{11} + a_{8n-4} d_{12} \quad (8(n-1) + 1)$$

$$a_{8n-5} = S_n d_{21} + a_{8n-4} d_{22} \quad (8(n-1) + 2)$$

and at the phase shifter

$$a_{8n-4} = a_{8n-5}(p_n)_{11} + a_{8n-2}(p_n)_{12} \quad (8(n-1) + 3)$$

$$a_{8n-3} = a_{8n-5}(p_n)_{21} + a_{8n-2}(p_n)_{22} \quad (8(n-1) + 4)$$

For coupler 2 through N-1

$$a_{8n-7} = \psi a_{8n-8}(c_n)_{11} + \psi a_{8n+1}(c_n)_{12} + a_{8n-3}(c_n)_{13} + a_{8n-1}\Gamma(c_n)_{14} \quad (8(n-1) + 5)$$

$$a_{8n} = \psi a_{8n-8}(c_n)_{21} + \psi a_{8n+1}(c_n)_{22} + a_{8n-3}(c_n)_{23} + a_{8n-1}\Gamma(c_n)_{24} \quad (8(n-1) + 6)$$

$$a_{8n-2} = \psi a_{8n-8}(c_n)_{31} + \psi a_{8n+1}(c_n)_{32} + a_{8n-3}(c_n)_{33} + a_{8n-1}\Gamma(c_n)_{34} \quad (8(n-1) + 7)$$

$$a_{8n-1} = \psi a_{8n-8}(c_n)_{41} + \psi a_{8n+1}(c_n)_{42} + a_{8n-3}(c_n)_{43} + a_{8n-1}\Gamma(c_n)_{44} \quad (8(n-1) + 8)$$

Finally, coupler N must be treated separately because of the extra load

$$a_{8N-7} = \psi a_{8N-8}(c_N)_{11} + a_{8N}\Gamma(c_N)_{12} + a_{8N-3}(c_N)_{13} + a_{8N-1}\Gamma(c_N)_{14} \quad (8N-3)$$

$$a_{8N} = \psi a_{8N-8}(c_N)_{21} + a_{8N}\Gamma(c_N)_{22} + a_{8N-3}(c_N)_{23} + a_{8N-1}\Gamma(c_N)_{24} \quad (8N-2)$$

$$a_{8N-2} = \psi a_{8N-8}(c_N)_{31} + a_{8N}\Gamma(c_N)_{32} + a_{8N-3}(c_N)_{33} + a_{8N-1}\Gamma(c_N)_{34} \quad (8N-1)$$

$$a_{8N-1} = \psi a_{8N-8}(c_N)_{41} + a_{8N}\Gamma(c_N)_{42} + a_{8N-3}(c_N)_{43} + a_{8N-1}\Gamma(c_N)_{44} \quad (8N)$$

The above 8N equations can be cast into matrix form

$$[S] = [F] [a]$$

where the vector $[S]$ contains the excitations $\{S_n\}$ and $[a]$ the unknowns $\{a_n\}$. $[F]$ is a feed scattering matrix obtained from the coefficients of the above equations. They can be represented as entries in the following table

		column = unknown index				
		a_1	a_2	a_3	a_{8N}
row = equation number	1					
	2					
	3					
	:					
	:					
	8N					

The matrix equation is solved to obtain $\{a_n\}$, and the reflection coefficients Γ_n in equation (5) can be calculated from $a_1, a_{10}, \dots, a_{8n-6}, \dots, a_{8N-6}$.

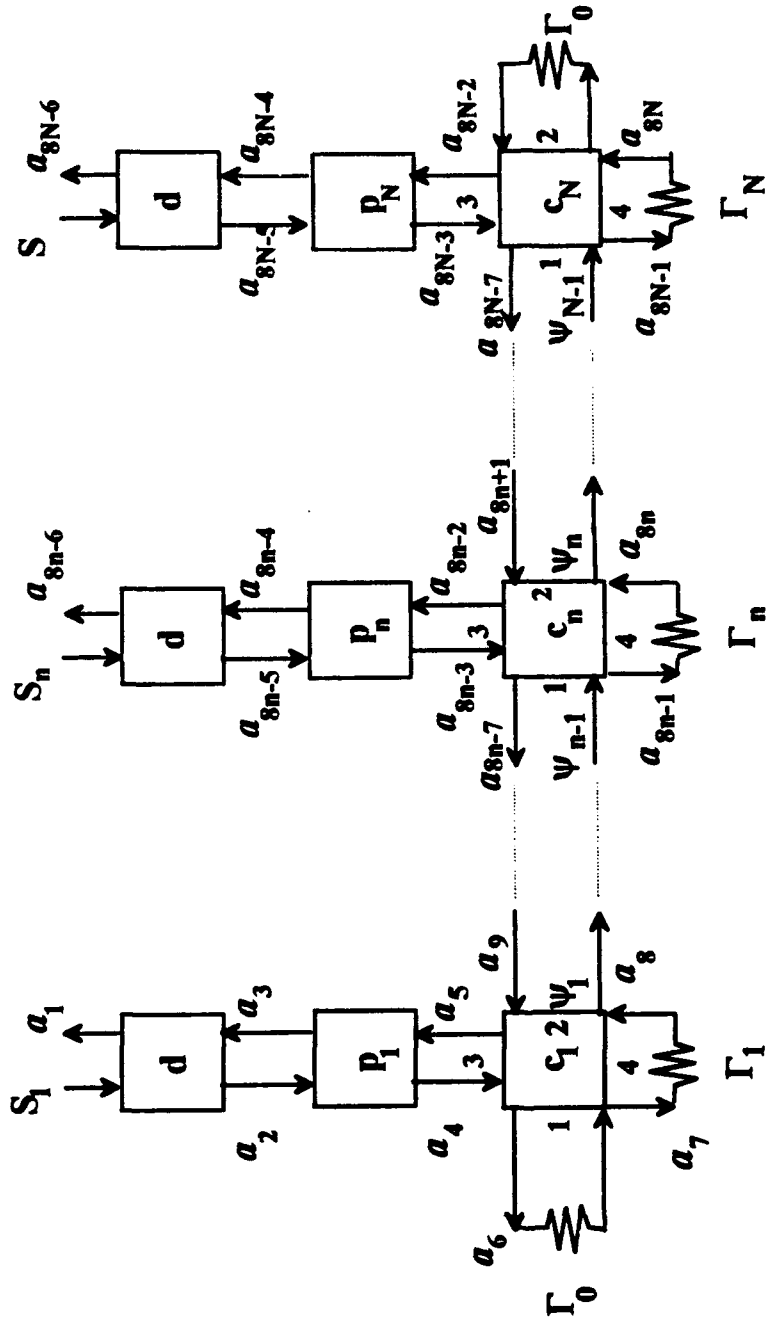


Figure C.1 : Scattering matrix feed diagram.

REFERENCES

- [1] C.G. Montgomery, R.H. Dicke and E.M. Purcell, *Principles of Microwave Circuits*, MIT Radiation Lab Series, vol. 8, McGraw-Hill, p. 317.
- [2] Y.Y. Hu, "Back-Scattering Cross Section of a Center-Loaded Antenna," *IRE Trans. on Antennas and Prop.*, vol. AP-6, no.1, January 1958, p. 140.
- [3] D. Midgley, "A Theory of Receiving Aerials Applied to the Reradiation of an Electro-magnetic Horn," *Proc. of IEEE*, vol. 108, Part B, no.42, November 1961, pp. 645~ 650.
- [4] N. Williams, "The RCS of Antennas - An Appraisal," *Military Microwaves Conference Proceedings*, Brighton, England, June 1986, pp. 505 ~ 508.
- [5] P.J. Tittensor and M.L. Newton, "Prediction of the Radar Cross Section of an Array Antenna," *Sixth International Conference on Antennas and Propagation*, London, England, April 1989, pp. 258 ~ 262.
- [6] V. Flokas, *Inband Scattering from Arrays with Parallel Feed Networks*, Master's Thesis, Naval Postgraduate School, June 1994.
- [7] R.C. Hansen, "Relationship between Antennas as Scatterers and as Radiators," *Proc. of the IEEE*, vol. 77, no. 5, May 1989, p. 659.
- [8] R.W.P. King and C.W. Harrison, "The Receiving Antenna," *Proc. of the IRE*, no. 32, January 1944, p. 35.
- [9] A.F. Stevenson, "Relations Between Transmitting and Receiving Properties of Antennas," *Quarterly of Appl. Math.*, vol. 5, January 1948, p. 140.
- [10] W.K. Kahn and H. Kurss, "Minimum-Scattering Antennas," *IEEE Trans. on Antennas and Prop.*, vol. AP-13, no. 5, September 1965, pp. 671 ~ 675.
- [11] R.B. Green, "Scattering from Conjugate-Matched Antennas," *IEEE Trans. on Antennas and Prop.*, vol. AP-14, no. 1, January 1966, p. 17.
- [12] D.C. Jenn, "Radar and Laser Cross Section Engineering," *Unpublished lecture notes*, Ch. 6.7, pp. 335.
- [13] D.C. Jenn, "Radar and Laser Cross Section Engineering," *Unpublished lecture notes*, Ch. 6.8, pp. 347 ~ 348.

INITIAL DISTRIBUTION LIST

- | | | |
|----|--|---|
| 1. | Defense Technical Information Center
Cameron Station
Alexandria, Virginia 22304-6145 | 2 |
| 2. | Library, Code 52
Naval Postgraduate School
Monterey, California 93943-5002 | 2 |
| 3. | Chairman, Code EW
Naval Postgraduate School
Monterey, California 93943-5002 | 1 |
| 4. | Jenn, D. C., Code EC/Jn
Naval Postgraduate School
Monterey, California 93943-5002 | 2 |
| 5. | Gill, G. S., Code EC/GL
Naval Postgraduate School
Monterey, California 93943-5002 | 1 |
| 6. | AC of S, G-2,
Republic of Korea Army Headquarters
Boonam-Ri, Dooma-Myun, Nonsan-Kun
Choong Nam, Korea | 1 |
| 7. | Lee, S. C.,
10329 Fernglen Ave.
Tujunga, CA 91042 | 1 |
| 8. | Lee, S. H.,
Dongdaemun-Gu, Hoegi-Dong 62-30
Seoul, Korea | 2 |